Solid State Reaction Study of the System Co-Li_2CO_3

A. Marini, V. Berbenni, V. Massarotti, D. Capsoni, and G. Bruni

Dipartimento di Chimica Fisica dell'Università di Pavia and CSTE-CNR, Viale Taramelli 16, I-27100 Pavia, Italy

Z. Naturforsch. **51a**, 813–820 (1996); received March 18, 1996

A detailed analysis of the reactive processes taking place in Co-Li_2CO_3 was performed by use of thermogravimetry and X-ray diffraction. A reaction model is proposed which accounts for the nature, stoichiometry, and amount of the phases present, at room temperature, in samples subjected to different thermal treatments. In particular it is shown that the thermal treatment influences substantially the final lithium content and the relative amount of the Li-containing phases. The results obtained for powdered samples are compared with those obtained in a previous work for plaques.

Key words: Cobalt oxides, Li-containing phases, stoichiometry, reaction model.

Introduction

A major problem in molten carbonate fuel cells is the stability of the cathode [1]. In [2] it was suggested that the stability of such cathodes my be improved by the use of cobalt-based materials, and it was argued that a likely candidate is solid Co-Li_2CO_3. In the present paper the reactive processes taking place in this promising system are analysed in detail.

1. Experimental

1.1 Products

Cobalt powder (Matthey, 99.8%, 1.6 μm) and lithium carbonate (Merck, 5671) were used as starting materials. The metal was used as supplied for pure cobalt samples. The other samples were obtained from mechanical mixtures of the reagents, carefully ground and stored at room temperature (rt.). The composition of the primary mixtures was $x_{Li} = 0.0974$ and $x_{Li} = 0.2017$ (x_{Li} = lithium cationic fraction). In the following these compositions will for simplicity be referred to as $x_{Li} = 0.10$ and $x_{Li} = 0.20$, respectively.

1.2 Apparatus and Procedures

1.2.1 Thermogravimetric Measurements

Thermogravimetric data were collected with a "Stanton Redcroft" 762 TGA thermobalance controlled by a "Rheometric Scientific" Thermal Analysis System. Unless otherwise noted, for the measurements samples weighting 30–40 mg were placed in a Pt-Rh crucible in air. Most of the measurements involved three steps:

1. **Heating** at 2 °C/min from rt. to a final temperature T_f in the range 900–1200 °C.
2. **Annealing** at T_f for between 0 and 5 hours.
3. **Cooling** down to rt. at 2 °C/min, unless otherwise marked.

After each run, the portion of sample recovered from the TGA pan (TG sample) was analyzed by XRD, and the results were correlated with the thermogravimetric information.

1.2.2 Diffractometric Measurements

XRD data were collected at rt. with a Philips PW 1710 diffractometer equipped with a Philips PW 1050 vertical goniometer and a graphite bent crystal monochromator, using the Cu $K\alpha$ radiation ($K\alpha_1$ = 1.5406 Å; $K\alpha_2$ = 1.5443 Å). A slice of a single crystal of silicon served as "sample holder": the TG samples (reground if necessary) were dispersed on its surface with the help of a few drops of acetone. Data were collected in the angular range $10° < 2\vartheta < 110°$ in the step scan mode (step = 0.03°, counting time = 1 s). The structural data and the relative amounts of the different phases were estimated by Rietveld refinement [3] with the programs DBW3-2S [4] and WYRIET, version 3.5 [5]. The stoichiometry of the phases was obtained from the TGA experiments (see below). For

Reprint requests to Prof. A. Marini.

0932-0784 / 96 / 0700-0813 $ 06.00 © – Verlag der Zeitschrift für Naturforschung, D-72072 Tübingen

each sample, the parameters were determined with a recursive least squares procedure. The sample displacement (zero order correction) was determined once, in the first run, while all other parameters were iteratively refined: in each run a new set of variables was added, and the refined parameters of the previous run were used as initial values. The sets of variables were:

1. scale factors, zero error (fixed in all the successive steps) and one coefficient for polynomial background;
2. lattice parameters;
3. three more coefficients for polynomial background;
4. profile parameter (u, w, y) and asymmetry for the pseudo Voigt profile function [6]; the variables involved in the Gaussian component of the profile and the asymmetry parameters were assumed to be the same for all the phases of the sample;
5. isotropic thermal factors for all the atoms; oxygen coordinates in the Co_3O_4 spinel [x, x, x(O)] and in the layered $LiCoCO_2$ structure [z(O)] [7].

The refinement of the preferred orientation parameter for the $h00$ planes of the CoO structure was carried out according to the March-Dollase equation [8], and was performed only for samples with the larger amounts of the disordered CoO-type phase. The orientation parameter and isotropic thermal factors of this disordered phase obtained from CoO-rich samples were used without refinement in the analysis of samples with low CoO content. The relative amounts of the different components were calculated following the procedure of Hill and Howard [9] and corrected for microabsorption effects.

2. Results and Discussion

2.1 TGA of Co Samples

Figure 1 shows a typical TGA curve of a pure Co sample. As shown in our previous work [2], the first product of oxidation is Co_3O_4, which transforms into CoO near 930 °C. From the trace it is clear that this transformation is reversible. The measured mass changes (percentages) at the different stages of the TGA curve (see Fig. 1) are: $m_1 - m_0 = 36.24 \pm 0.23$; $m_2 - m_1 = -8.96 \pm 0.14$; $m'_1 - m'_2 = 8.95 \pm 0.13$. These should be compared with those expected for the transformations $Co \rightarrow Co_3O_4 \rightarrow CoO \rightarrow Co_3O_4$ which are 36.20 and ± 9.05 respectively. The very good agreement between the TGA data and the weight changes evaluated according to this reaction scheme shows that the reactions yield stoichiometric products.

2.2 TGA of Li-containing Samples

A typical TGA plot of a lithium containing sample is shown in Figure 2. The weight initially increases because of the Co oxidation; before the $Co_3O_4 \rightarrow CoO$ transformation takes place, the weight decreases due to decomposition of Li_2CO_3. The weight decreases also during the annealing at T_f; the amount of decrease depends upon the sample composition and becomes larger with increasing temperature (T_f) and duration (t) of the annealing.

A careful quantitative analysis is needed to identify the products present at the various plateaux of the TGA run, where the weights are m_1, m_2, m_3, and m_4 (see Figure 2). For convenience, all the weights will be

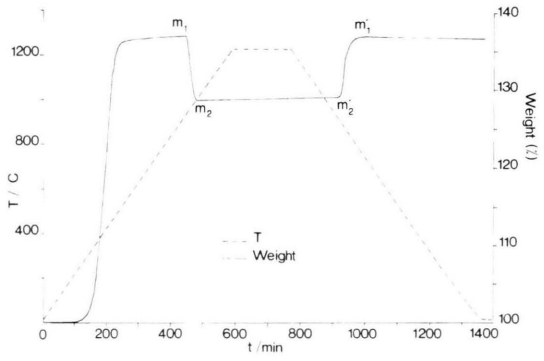

Fig. 1. TGA curve and temperature profile of a pure Co sample.

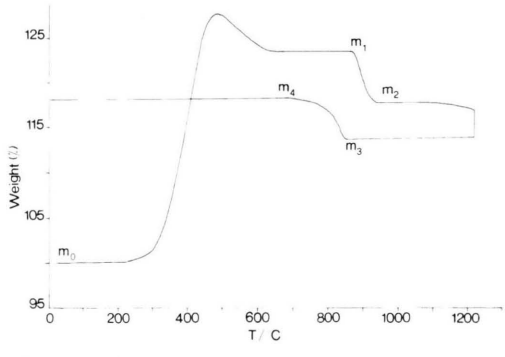

Fig. 2. Typical TGA curve of a Li-containing sample ($x_{Li} = 0.20$).

scaled to an initial weight $m_0 = 100$ g, and the same symbol will represent either these weights or the stage where they are determined.

X-ray data show that at stage m_1 only two phases are present: Co_3O_4 and $LiCoO_2$. The weight change $m_1 - m_0$ may be calculated assuming complete transformation of Co into Co_3O_4, quantitative $LiCoO_2$ formation, and complete Li_2CO_3 decomposition. The reactions which determine m_1 are the following:

$$2n[(1 - x_{Li})/x_{Li}]\,Co + (4/3)n[(1 - x_{Li})/x_{Li}]\,O_2 \rightarrow (2/3)n[(1 - x_{Li})/x_{Li}]\,Co_3O_4\,, \quad (1)$$

$$n\,Li_2CO_3 \rightarrow n\,Li_2O + n\,CO_2\,, \quad (2)$$

$$n\,Li_2O + (2/3)n\,Co_3O_4 + (n/6)\,O_2 \rightarrow 2n\,LiCoO_2\,. \quad (3)$$

The coefficient n was added as a factor normalizing to 100 g of starting mixture (n represents the moles of Li_2CO_3 in 100 g of the starting mixture). By interpreting the chemical formulas as the corresponding molecular weights, the reaction equations become stoichiometric relationships which yield directly the calculated weights m_{icalc}.

The weight decrease from m_1 to m_2 (see Fig. 2) is due to transformation of the Co_3O_4 left by reaction (3) into CoO:

$$(2/3)n[(1 - 2x_{Li})/x_{Li}]\,Co_3O_4 \rightarrow 2n[(1 - 2x_{Li})/x_{Li}] \cdot CoO + (n/3)[(1 - 2x_{Li})/x_{Li}]\,O_2\,. \quad (4)$$

The weight changes calculated for (1)–(4) are reported in Table 1. The experimental values of $m_1 - m_0$ and $m_2 - m_1$ have been obtained as the mean of at least ten independent measurements and are 30.20 ± 0.34 and -7.56 ± 0.11, respectively, for $x_{Li} = 0.10$ and 23.56 ± 0.31, and -5.82 ± 0.08 for $x_{Li} = 0.20$. While computed and experimental values of $m_2 - m_1$ are perfectly consistent, the experimental $m_1 - m_0$ values are slightly lower than the calculated ones. Very likely this is due to an oxygen deficiency of $LiCoO_2$, which will be henceforth written as $LiCoO_{2-x}$. Consequently, (3) must be rewritten as

$$n\,Li_2O + (2/3)n\,Co_3O_4 + n[(1/6) - x]\,O_2 \rightarrow 2n\,LiCoO_{2-x}\,. \quad (3')$$

The mean values of x can be obtained from the equation

$$m_{1,\,calc} - m_1 = n\,x\,O_2\,,$$

Table 1. Li-containing samples. Calculated mass changes (percentages) for Eq. (1), (2), (3), and (4) (see text).

	$x_{Li} = 0.10$	$x_{Li} = 0.20$
$\Delta m_1 = [(4/3)n(1 - x_{Li})/x_{Li}]\,O_2$	33.90	31.25
$\Delta m_2 = -nCO_2$	−3.77	−8.15
$\Delta m_3 = (n/6)\,O_2$	0.46	0.99
$m_{1calc} - m_0 = \Delta m_1 + \Delta m_2 + \Delta m_3$	30.59	24.09
$m_{2calc} - m_{1calc} = \Delta m_4 = [-(n/3)(1 - 2x_{Li})/x_{Li}]O_2$	−7.56	−5.84

Table 2. Pure Co samples: lattice constants and mass percentages by X-ray analysis.

Thermal treatment		CoO		Co_3O_4	
T_f/°C	•t/h	%	lattice const. a/Å	%	lattice const. a/Å
1100	1	–	–	100	8.082
1100	3	–	–	100	8.083
1100	5	0.83	4.253	99.17	8.082
1200	1	3.72	4.257	96.28	8.087
1200	3	11.30	4.250	88.70	8.085
1200*	5	56.13	4.254	43.87	8.086
			4.254 ± 0.003		8.084 ± 0.002

* cooling rate = 50 °C/min; • annealing time.

from which it follows

$$x = 0.14 \quad \text{for} \quad x_{Li} = 0.10\,,$$
$$x = 0.09 \quad \text{for} \quad x_{Li} = 0.20\,.$$

These values of x have been used in the X-ray refinement.

Equations (1), (2), (3′), and (4) describe the first heating step of the TGA run for Li-containing samples. Before analysing the annealing and cooling stages of these samples, we discuss the XRD findings.

2.3 XRD of Pure Co Samples

Table 2 lists compositions and lattice parameters of Co samples subjected to different thermal cycles. In the experiment with 3 h annealing at 1100 °C, only the Co_3O_4 phase is present at the end. Traces of CoO begin to appear with $t = 5$ h and $T_f = 1100$ °C. With $T_f = 1200$ °C, the fraction of CoO is appreciable after 1 h annealing and increases on increasing t and the cooling rate. Such a behaviour is consistent with that found on cobalt based plaques [2], and confirms that not all the CoO, which is the only phase at T_f, reverts

to Co_3O_4 during cooling; either the degree of sinterization is too high, or the cooling rate too fast to let the oxygen penetrate the bulk of the grains.

2.4 XRD of Li-containing Samples

The results of the X-ray refinement of the samples with lithium are summarised in Tables 3 and 4. Within the experimental error, the lattice constants of Co_3O_4 are the same for $x_{Li} = 0.10$, $x_{Li} = 0.20$, and for pure Co samples. This result is reinforced by the TGA data, which imply that stoichiometric Co_3O_4 is always obtained at rt., independently of the Li content.

The lattice parameter of the CoO phase takes appreciably different values for $x_{Li} = 0.10$, $x_{Li} = 0.20$, and the Co samples. We may assume that a solid solution of the type $Li_yCo_{1-y}O$, rather than the "pure" CoO, may be obtained when lithium is present, and that the CoO lattice parameter decreases monotonically with y. If this is the case, it can be deduced from Tables 3 and 4 that the composition of this solid solution depends on x_{Li}, but not on the thermal treatment. Furthermore, since the $x_{Li} = 0.10$ samples have the smallest lattice parameter, they have also the highest y value [10]. As stated before, the samples with lithium contain also a non-stoichiometric $LiCoO_{2-x}$ phase, where the oxygen deficit (x) was determined to be higher for the $x_{Li} = 0.10$ than for the $x_{Li} = 0.20$ samples. This is probably not a case and suggests that the x and y are essentially the same.

The final lithium fraction $\bar{x}_{Li,f}$, correlates, positively and strongly, with the fraction of $LiCoCO_{2-x}$. Such a linkage is particularly evident in the $x_{Li} = 0.20$ samples (Table 4). Obviously, a final Li fraction smaller than the initial one means that an appreciable amount of lithium has volatilized; consequently, also the per-

Table 3. Li-containing samples ($x_{Li} = 0.10$). Lattice constants, mass percentages and final lithium cationic fraction by X-ray analysis.

Thermal treatment		CoO ($Li_{0.14}Co_{0.86}O$)		Co_3O_4		$LiCoO_{1.86}$	$\bar{x}_{Li,f}$
T_f/°C	•t/h	%	lattice const. a/Å	%	lattice const. a/Å	%	
1100	1	–	–	86.66	8.079	13.34	0.100
1100	3	–	–	86.70	8.083	13.30	0.100
1100	5	3.86	4.216	84.75	8.080	11.39	0.096
1200	1	1.51	4.222	86.57	8.083	11.92	0.095
1200	3	7.18	4.220	81.57	8.083	11.25	0.100
1200	5	4.73	4.220	86.19	8.084	9.08	0.076
			4.219 ± 0.002		8.082 ± 0.002		

• annealing time.

Table 4. Li-containing samples ($x_{Li} = 0.20$). Lattice constants, mass percentages and final lithium cationic fraction by X-ray analysis.

Thermal treatment		CoO ($Li_{0.09}Co_{0.91}O$)		Co_3O_4		$LiCoO_{1.91}$	$\bar{x}_{Li,f}$
T_f/°C	•t/h	%	lattice const. a/Å	%	lattice const. a/Å	%	
650	–	–	–	73.03	8.082	26.97	0.184
800	–	–	–	68.48	8.080	31.52	0.217
865	–	–	–	68.18	8.085	31.82	0.218
950	–	–	–	71.24	8.083	28.76	0.201
1100	1	–	–	67.23	8.079	32.77	0.233
1100	3	1.02	4.234	73.94	8.083	25.04	0.179
1100	5	7.92	4.232	69.32	8.082	22.76	0.169
1200	–	2.15	4.234	75.56	8.083	22.29	0.163
1200	1	8.25	4.230	71.82	8.082	19.93	0.151
1200	3	19.32	4.231	65.73	8.086	14.95	0.126
1200	5	29.48		61.37		9.15	0.093
			4.232 ± 0.002		8.082 ± 0.002		

• annealing time.

centage of $LiCoO_{2-x}$ should be smaller than expected. It is worth noting in Table 4 that, when $T_f = 1200\,°C$, the $LiCoO_{2-x}$ fraction decreases with the annealing time, while the $Li_yCo_{1-y}O$ phase increases. This suggests that $Li_yCo_{1-y}O$, forms as a result of the decomposition of $LiCoO_{2-x}$.

2.5 TGA of Li-containing Samples During Annealing

In discussing Fig. 2, we remarked that a weight loss takes place during annealing, which is related with x_{Li}, but also with T_f and t. The XRD evidence suggests that the weight decrease is due to loss of Li_2O. If we put $x = y$, as suggested by our data, and assume that the only process responsible for $Li_yCo_{1-y}O$ formation is decomposition of $LiCoO_{2-x}$, we can write

$$\begin{aligned} 2n\alpha\,LiCoO_{2-x} \rightarrow\ & [(2n\alpha)/(1-x)]\,Li_xCo_{1-x}O \\ & + [2n\alpha(1-2x)/2(1-x)\,Li_2O \\ & + 2n\alpha[(2(1-x)^2-1)/4(1-x)]\,O_2\,, \end{aligned} \tag{5}$$

where α is a coefficient ($0 \leq \alpha \leq 1$). Therefore, if $Li_xCo_{1-x}O$ formation takes place, according to this scheme, the weight decrease at T_f is due to loss of Li_2O and oxygen.

The process occurring during the cooling to rt. is only the $CoO \rightarrow Co_3O_4$ transformation:

$$\begin{aligned} 2n[(1-2x_{Li})/x_{Li}]\,CoO + (n/3)[(1-2x_{Li})/x_{Li}]\,O_2 \\ \rightarrow (2n/3)[(1-2x_{Li})/x_{Li}]\,Co_3O_4\,. \end{aligned} \tag{6}$$

Equations (5) and (6), together with (1), (2), (3′), and (4), describe what in the following will be called "reaction model A". According to this model, the amount of the Co_3O_4 phase in the rt. samples depends upon the initial composition, and not upon the thermal treatment. However, Tables 3 and 4 show that this is true only approximately. With model A and the TGA data at the end of annealing we may compute $\bar{x}_{Li,f}$ and the final fractions for all phases. The results are listed in Tables 5 and 6, along with the values experimentally determined through X-ray refinement. The agreement is acceptable for a gentle annealing, but the model gives an underestimate of the $Li_xCo_{1-x}O$ fraction determined by X-ray, which is the larger the higher T_f and the longer t. Such a behaviour suggests that this phase can be formed from $LiCoO_{2-x}$ decomposition, as per model A, and also by the solid state reaction

$$\begin{aligned} 2n\beta\,LiCoO_{2-x} + 2n\beta[(1-2x)/x]\,CoO \\ + n\beta x\,O_2 \rightarrow (2n\beta/x)\,Li_xCo_{1-x}O\,, \end{aligned} \tag{7}$$

where β is a coefficient ($0 \leq \beta \leq 1$). If an α fraction of the $LiCoO_{2-x}$ phase reacts according to (5) and a β fraction according to (7), the total reaction during annealing will simply be the sum of (5) and (7), i.e.

$$\begin{aligned} 2n(\alpha+\beta)\,LiCoO_{2-x} + 2n\beta[(1-2x)/x]\,CoO \\ \rightarrow 2n[(\beta/x) + \alpha/(1-x)]\,Li_xCo_{1-x}O \\ + [n\alpha(1-2x)/(1-x)]\,Li_2O \\ + n\{[\alpha(2(1-x)^2-1)/2(1-x)] - \beta x\}\,O_2\,. \end{aligned} \tag{8}$$

Since the CoO which has formed $Li_xCo_{1-x}O$ at high temperature will not transform to Co_3O_4 during cooling, the reaction taking place in going from T_f to rt. should be written as

$$\begin{aligned} 2n\{[(1-2x_{Li})/x_{Li}] - \beta(1-2x)/x\}\,CoO \\ + (n/3)\{[(1-2x_{Li})/x_{Li}] - \beta(1-2x)/x\}\,O_2 \\ \rightarrow (2n/3)\{[(1-2x_{Li})/x_{Li}] - \beta(1-2x)/x\}\,Co_3O_4\,. \end{aligned} \tag{9}$$

The model described by (8) and (9) [together with (1), (2), (3′), and (4)] will be referred to as "reaction model A*". The value of β can be obtained from the weight changes during cooling ($m_4 - m_3$), while α from the weight changes during annealing ($m_3 - m_2$), if β is already known. With α and β, one can compute the final fractions of all phases, and the final lithium content. The parameters of models A and A* are summarized in Tables 5 ($x_{Li} = 0.10$) and 6 ($x_{Li} = 0.20$).

2.6 Comparison Between the Reaction Models

The need to introduce (7) came from the worsening of the agreement between model A and the experimental data when T_f and t increase. As a consequence, the two models present almost the same reaction picture at the lowest T_f and shortest t (Tables 5.1, 5.2 and 6.1, 6.2). On the other hand, only model A* is compatible with the XRD findings for samples annealed at 1200 °C for more than 1 h; in other words, the role of the reaction (7) in the production of $Li_xCo_{1-x}O$ becomes substantial as the annealing temperature and time are increased. Model A* can be used to calculate the percentage of $Li_xCo_{1-x}O$ obtained by solid state reaction at $T_f = 1200\,°C$ and in the $x_{Li} = 0.20$ samples which yield a relatively high $Li_xCo_{1-x}O$ fraction (Tables 6.4, 6.5 and 6.6). Thus, for the isothermal annealing times of 1 h, 3 h and 5 h, the percentages of the $Li_xCo_{1-x}O$ fraction obtained by solid state reaction were evaluated as 29%, 57% and 48%, respectively.

The amount of $Li_xCo_{1-x}O$ produced is not related in a simple way with the weights α and β of the two

Table 5. Li-containing samples ($x_{Li} = 0.10$). Quantitative parameters by thermogravimetric analysis according to models A and A* (see text). Data from X-ray analysis are reported for comparison.

	α	β	m_{calc}	m_{meas}	% $Li_xCo_{1-x}O$	% $LiCoO_{2-x}$	% Co_3O_4	$\bar{x}_{Li,f}$
5.1: $T_f = 1100\,°C$; $t = 1\,h$; $m_3 - m_2 = -0.19$; $m_4 - m_3 = 7.50$.								
Model A	0.066	–	130.00	130.40	0.68	11.78	87.53	0.092
Model A*	0.067	0.013	129.95	130.40	1.54	11.60	86.86	0.092
X-ray	–	–	–	–	0.00	13.34	86.66	0.103
5.2: $T_f = 1100\,°C$; $t = 3\,h$; $m_3 - m_2 = -0.26$; $m_4 - m_3 = 7.52$.								
Model A	0.090	–	129.94	129.91	0.93	11.48	87.58	0.091
Model A*	0.091	0.009	129.90	129.91	1.51	11.36	87.13	0.091
X-ray	–	–	–	–	0.00	13.30	86.70	0.103
5.3: $T_f = 1100\,°C$; $t = 5\,h$; $m_3 - m_2 = -0.30$; $m_4 - m_3 = 7.35$.								
Model A	0.104	–	129.90	129.24	1.08	11.31	87.61	0.090
Model A*	0.110	0.046	129.68	129.24	4.03	10.67	85.30	0.089
X-ray	–	–	–	–	3.86	11.39	84.75	0.096
5.4: $T_f = 1200\,°C$; $t = 1\,h$; $m_3 - m_2 = 0.0$; $m_4 - m_3 = 7.40$.								
Model A	0.000	–	130.20	129.95	0.00	12.59	87.41	0.097
Model A*	0.005	0.035	130.03	129.95	2.24	12.10	85.60	0.097
X-ray	–	–	–	–	1.51	11.92	86.57	0.097
5.5: $T_f = 1200\,°C$; $t = 3\,h$; $m_3 - m_2 = -0.35$; $m_4 - m_3 = 7.12$.								
Model A	0.121	–	129.85	129.33	1.26	11.10	87.64	0.088
Model A*	0.134	0.096	129.40	129.33	7.43	9.76	82.81	0.087
X-ray	–	–	–	–	7.18	11.25	81.57	0.100
5.6: $T_f = 1200\,°C$; $t = 5\,h$; $m_3 - m_2 = -0.77$; $m_4 - m_3 = 7.40$.								
Model A	0.266	–	129.43	129.06	2.78	9.30	87.93	0.077
Model A*	0.271	0.035	129.27	129.06	5.04	8.81	86.16	0.077
X-ray	–	–	–	–	4.73	9.08	86.19	0.080

Note to Tables 5 and 6:
α = fraction of the $LiCoO_{2-x}$ phase that reacts according to (5) (see text);
β = fraction of the $LiCoO_{2-x}$ phase that reacts according to (7) (see text);
m_{calc} and m_{meas} are the calculated and measured final masses, respectively.
For each sample are also reported:
T_f, t = temperature and time of the isothermal stage, respectively;
$m_3 - m_2$ = percentage mass loss during the annealing isothermal stage;
$m_4 - m_3$ = percentage mass gain during sample cooling.

reactions (5) and (7); for example, with $x_{Li} = 0.20$ identical amounts of $Li_xCo_{1-x}O$ are produced by decomposition and by solid state reaction, when $\beta \cong 0.10\,\alpha$, although for $t = 5$ h, the percentage obtained by solid state reaction is slightly smaller than for $t = 3$ h. However, this is not in contradiction with the trend of a declining role of decomposition on increasing t, because the 3 h long annealing was not performed in air, as all other runs, but under N_2 flux and a negligible oxygen partial pressure. Under these conditions the only oxygen source is $LiCoO_{2-x}$ decomposition [reaction (5)].

The above remarks, and the fact that excellent agreement between the total weights measured at the end of the experiments and the calculated final weight is obtained with model A*, but no so with model A, apparently support both the correctness of the refinement procedure and the validity of reaction model A*.

3. Comments

3.1 X-ray Data

The $\bar{x}_{Li,f}$ values obtained by model A* are generally in good agreement with those obtained by X-ray data. However, the latter are generally slightly greater than the former, and it is very likely that the X-ray data slightly overestimate this parameter. This is seen in the

Table 6. Li-containing samples ($x_{Li} = 0.20$). Quantitative parameters by thermogravimetric analysis according to models A and A* (see text). Data from X-ray analysis are reported for comparison.

	α	β	m_{calc}	m_{meas}	% $Li_xCo_{1-x}O$	% $LiCoO_{2-x}$	% Co_3O_4	$\bar{x}_{Li,f}$
6.1: $T_f = 1100\,°C$; $t = 1\,h$; $m_3 - m_2 = -0.64$; $m_4 - m_3 = 5.83$.								
Model A	0.090	–	122.92	122.75	2.09	26.44	71.47	0.188
Model A*	0.090	0.000	122.91	122.75	2.18	26.43	71.39	0.188
X-ray	–	–	–	–	0.00	32.77	67.23	0.233
6.2: $T_f = 1100\,°C$; $t = 3\,h$; $m_3 - m_2 = -1.10$; $m_4 - m_3 = 5.80$.								
Model A	0.154	–	122.46	122.80	3.60	24.66	71.74	0.179
Model A*	0.154	0.002	122.42	122.80	4.09	24.60	71.30	0.179
X-ray	–	–	–	–	1.02	25.04	73.94	0.179
6.3: $T_f = 1100\,°C$; $t = 5\,h$; $m_3 - m_2 = -1.50$; $m_4 - m_3 = 5.65$.								
Model A	0.210	–	122.06	122.05	4.93	23.09	71.98	0.170
Model A*	0.211	0.010	121.87	122.05	7.42	22.80	69.77	0.170
X-ray	–	–	–	–	7.92	22.76	69.32	0.169
6.4: $T_f = 1200\,°C$; $t = 1\,h$; $m_3 - m_2 = -2.36$; $m_4 - m_3 = 5.60$.								
Model A	0.331	–	121.20	121.30	7.80	19.70	72.50	0.151
Model A*	0.332	0.013	120.96	121.30	10.99	19.33	69.68	0.150
X-ray	–	–	–	–	8.25	19.93	71.82	0.151
6.5: $T_f = 1200\,°C$; $t = 3\,h$; $m_3 - m_2 = -2.92$; $m_4 - m_3 = 4.86$.								
Model A	0.410	–	120.64	119.56	9.70	17.47	72.82	0.137
Model A*	0.414	0.054	119.66	119.56	22.99	15.88	61.12	0.137
X-ray	–	–	–	–	19.32	14.95	65.73	0.126
6.6: $T_f = 1200\,°C$; $t = 5\,h$; $m_3 - m_2 = -5.07$; $m_4 - m_3 = 4.64$.								
Model A	0.711	–	118.49	117.14	17.10	8.70	74.10	0.083
Model A*	0.716	0.066	117.29	117.14	33.80	6.60	59.54	0.082
X-ray	–	–	–	–	29.48	9.15	61.37	0.093

cases of Tables 5.1, 5.2 and 5.3, where the nominal lithium content is $x_{Li} = 0.0974$, and in the case of Table 6.1, where the nominal lithium content is $x_{Li} = 0.2017$. It can be seen in the pertinent tables that, where $\bar{x}_{Li,f}$ is overestimated, the $LiCoO_{2-x}$ mass percentage by X-ray is appreciably greater than that of model A*. In other words, there appears to be a tendency of X-ray refinement to overestimate the amount of the $LiCoO_{2-x}$ phase. The same trend was found in our previous paper [2], where an explanation of such a behaviour was proposed.

3.2 $LiCoO_{2-x}$ and $Li_xCo_{1-x}O$ Stoichiometry

TGA yields direct evidence for the non-stoichiometry of $LiCoO_{2-x}$ and for the different x values with different nominal composition. A trend in the lattice constants of $Li_xCo_{1-x}O$ points to the non-stoichiometry of this phase. However, there is not a direct evidence that the x value is the same in $LiCoO_{2-x}$ and $Li_xCo_{1-x}O$. In fact, TGA can not be used to calculate the x value of $Li_xCo_{1-x}O$ because both the relative amount and the stoichiometry of such a phase are unknown, and only one of these parameters can be obtained from thermogravimetric data. On the X-ray side, the role of x in the refinement is too small to allow such an estimation to be made with XRD. The assumption that the parameter of non-stoichiometry has the same value in $LiCoO_{2-x}$ and $Li_xCo_{1-x}O$ is proven by the trend of the lattice constants. If substitution of Li for Co in the cationic sublattice of CoO leads to a shorthening of the lattice constant proportional to the lithium content, as it occurred in the case of $Li_xNi_{1-x}O$ [10], the relationship should be

$$a_{LixCo1-xO} = a_{CoO} - K\,x\,,$$

i.e. $$K = (a_{CoO} - a_{LixCo1-xO})/x\,,$$

and the same K value is obtained for both x values. Thus the values of the lattice constants confirm that

the x values of the $Li_xCo_{1-x}O$ phases, obtained from samples of nominal lithium content $x_{Li} = 0.10$ and 0.20, are exactly in the ratio 0.14/0.09, as deduced from TGA measurements.

The reason why the x value of the $LiCoO_{2-x}$ phase is higher when $x_{Li} = 0.10$ than when $x_{Li} = 0.20$, is presently not clear. We suspect that there might be an epitaxial growth of the $LiCoO_2$ phase on the Co_3O_4 phase, becoming less important when the nominal lithium content increases. Work is in progress to understand this point.

The fact that pure CoO transforms into Co_3O_4 during cooling and that $Li_xCo_{1-x}O$ and CoO have exactly the same structure must be stressed. Another important point of the model is that $Li_xCo_{1-x}O$ is stable and does not transform during cooling. Thus, the presence of about 10% of Co(III) atoms is able to avoid the transformation of CoO into Co_3O_4.

3.3 Plaques and Powders

The results obtained in the present work for pure Co samples are completely consistent with the behaviour described for pure Co plaques [2]. In that case, however, in Li-containing samples a highly non-stoichiometric Co_3O_4 phase was present, while here the Co_3O_4 phase is stoichiometric. The major difference stems from the weight changes measured in plaques and powders. Upon heating up to $T_f = 800 \div 900\,^\circ C$, the weight change of plaques was by $15.3\% \div 14.3\%$ lower than calculated for $x_{Li} = 0.10$ and $x_{Li} = 0.20$, respectively. After thermal cycling the powders at T_f in the 800–900 °C range, the weight gain is only 0.6% and 2.6% lower than calculated for the $x_{Li} = 0.10$ and $x_{Li} = 0.20$ samples, respectively. It is apparent that powders show a much higher weight increase than plaques do. A binder and an antifoaming agent were mixed to Co and Li_2CO_3 to obtain plaques. The burnout of these organic substances can be considered complete around 500 °C. Since our measurements show that the Co → Co_3O_4 reaction completes around this temperature (see Figs. 1 and 2), it follows that Co_3O_4 formation occurs in plaques, during the organic substances burnout. However, this release does not exert any effect on pure Co plaques; after treatment at $T_f = 800\,^\circ C$ and $T_f = 900\,^\circ C$, they showed exactly the weight gain expected as the powdered samples do. On the contrary, it is apparent that the presence of the organic substances affects the behaviour of Li-containing plaques, probably via an early formation of $LiCoO_2$. This might occur because, unlike powders, the plaque becomes quite uniformly covered by $LiCoO_2$ during Co oxidation, thus hindering oxygen diffusion into the sample and causing incomplete cobalt oxidation to the Co(III) status, and the appearance of oxygen defects. In other words it is likely that the main effect of the burnout of organic substances is to anticipate the Li_2CO_3 decomposition, and then the $LiCoO_2$ formation. This suggests that trying to transfer the knowledge from one system to a similar one may be a tricky business.

Acknowledgements

This work has been supported by MURST 40% funds and CSGI.

[1] N. Q. Minh, J. Power Sources **24,** 1 (1988).
[2] A. Marini, V. Berbenni, V. Massarotti, D. Capsoni, and E. Antolini, J. Solid State Chem. **116,** 15 (1995).
[3] H. M. Rietveld, J. Appl. Crystallogr. **2,** 65 (1969).
[4] D. B. Wiles and R. A. Young, J. Appl. Crystallogr. **14,** 149 (1981).
[5] J. Schneider, IUCR Int. Workshop on the Rietveld Method, Petten (1989).
[6] P. Thompson, D. E. Cox, and J. B. Hastings, J. Appl. Cryst. **20,** 79 (1987).
[7] W. D. Johnston, R. R. Heike, and D. Sestrick, J. Phys. Chem. Solids **7,** 1 (1958).
[8] W. A. Dollase, J. Appl. Crystallogr. **19,** 267 (1986).
[9] R. J. Hill and C. J. Howard, J. Appl. Crystallogr. **20,** 467 (1987).
[10] E. Antolini, M. Leonini, V. Massarotti, A. Marini, V. Berbenni, and D. Capsoni, Solid State Ionics **39,** 251 (1990).